university of groningen

University Medical Center Groningen

University of Groningen

The oligomeric distribution of SecYEG is altered by SecA and translocation ligands

Scheuring, J; Braun, N; Nothdurft, L; Stumpf, M; Veenendaal, AKJ; Kol, S; van der Does, C; Driessen, Arnold; Weinkauf, S; Veenendaal, Andreas K.J.

Published in:
Journal of Molecular Biology

DOI:
10.1016/j.jmb.2005.09.058

IMPORTANT NOTE: You are advised to consult the publisher's version (publisher's PDF) if you wish to cite from it. Please check the document version below.

Document Version
Publisher's PDF, also known as Version of record

Publication date:
2005

Link to publication in University of Groningen/UMCG research database

Citation for published version (APA):
Scheuring, J., Braun, N., Nothdurft, L., Stumpf, M., Veenendaal, A. K. J., Kol, S., ... Veenendaal, A. K. J. (2005). The oligomeric distribution of SecYEG is altered by SecA and translocation ligands. Journal of Molecular Biology, 354(2), 258-271. DOI: 10.1016/j.jmb.2005.09.058

Copyright
Other than for strictly personal use, it is not permitted to download or to forward/distribute the text or part of it without the consent of the author(s) and/or copyright holder(s), unless the work is under an open content license (like Creative Commons).

Take-down policy
If you believe that this document breaches copyright please contact us providing details, and we will remove access to the work immediately and investigate your claim.

Downloaded from the University of Groningen/UMCG research database (Pure): http://www.rug.nl/research/portal. For technical reasons the number of authors shown on this cover page is limited to 10 maximum.

Download date: 10-02-2018

doi:10.1016/j.jmb.2005.09.058 J. Mol. Biol. (2005) 354, 258–271

JMB

Available online at www.sciencedirect.com

SCIENCE DIRECT®

ELSEVIER

The Oligomeric Distribution of SecYEG is Altered by SecA and Translocation Ligands

Johannes Scheuring[1], Nathalie Braun[1], Lars Nothdurft[1] Matthias Stumpf[1], Andreas K. J. Veenendaal[2], Stefan Kol[2] Chris van der Does[2], Arnold J. M. Driessen[2] and Sevil Weinkauf[1]*

[1]*Department of Chemistry Technical University Munich Lichtenbergstr. 4, 85747 Garching, Germany*

[2]*Department of Microbiology University of Groningen Kerklaan 30, 9751 NN Haren The Netherlands*

**Corresponding author*

The multimeric membrane protein complex translocase mediates the transport of preproteins across and integration of membrane proteins into the inner membrane of *Escherichia coli*. The translocase consists of the peripheral membrane-associated ATPase SecA and the heterotrimeric channel-forming complex consisting of SecY, SecE and SecG. We have investigated the quaternary structure of the SecYEG complex in proteoliposomes. Fluorescence resonance energy transfer demonstrates that SecYEG forms oligomers when embedded in the membrane. Freeze-fracture techniques were used to examine the oligomeric composition under non-translocating and translocating conditions. Our data show that membrane-embedded SecYEG exists in a concentration-dependent equilibrium between monomers, dimers and tetramers, and that dynamic exchange of subunits between oligomers can occur. Remarkably, the formation of dimers and tetramers in the lipid environment is stimulated significantly by membrane insertion of SecA and by the interaction with translocation ligands SecA, preprotein and ATP, suggesting that the active translocation channel consists of multiple SecYEG complexes.

© 2005 Elsevier Ltd. All rights reserved.

Keywords: electron microscopy; preprotein translocation; SecYEG; translocase; oligomerization

Introduction

Transport of the majority of preproteins across and integration of membrane proteins into the cytoplasmic membrane of *Escherichia coli* is mediated by a multisubunit complex termed translocase. Translocase consists of a protein-conducting channel formed by the heterotrimeric membrane complex SecYEG and the peripheral membrane-associated, homodimeric ATPase SecA.[1–4] SecYEG-associated SecA serves as membrane receptor for preproteins. Translocation is initiated by the binding of ATP to the SecYEG- and preprotein-bound SecA.[5] This process triggers a conformational change in SecA that facilitates the translocation of a preprotein segment across the membrane, whereupon the preprotein is released from SecA in a step that requires ATP hydrolysis.[6] Consecutive cycles of ATP binding and hydrolysis coupled to preprotein binding and release result in the stepwise translocation of the polypeptide chain through the aqueous channel formed by SecYEG.[7] The observation that the translocating preprotein is in contact mainly with SecA and SecY, and is shielded from phospholipids,[8] and the fact that domains of SecA are protease-resistant during translocation,[5,9] led to the hypothesis of a partial co-insertion of SecA into the membrane or translocation pore. According to the membrane insertion model,[5] SecA cycles in an ATP-dependent manner in and out of the translocation channel, allowing the successive movement of the preprotein through the

Present addresses: L. Nothdurft, SAS Hagmann, Weberstrasse 3, Horb a. N., Germany; M. Stumpf, Tietz Video and Image Processing Systems GmbH, Eremitenweg 1, 82131 Gauting, Germany; C. van der Does, Johann Wolfgang Goethe-Universität, Frankfurt am Main, Institute of Biochemistry, Biocenter, Marie Curie Strasse 9, 60439 Frankfurt, Germany.

Abbreviations used: FRET, fluorescence resonance energy transfer; LPR, lipid to protein ratio; MRA, multi reference alignment; MSA, multivariate statistical analysis.

E-mail address of the corresponding author: sevil.weinkauf@ch.tum.de

0022-2836/$ - see front matter © 2005 Elsevier Ltd. All rights reserved.

membrane; here, this is referred to as membrane-inserted SecA. Auxiliary proteins that are involved in translocation are the heterotrimeric membrane complex SecDFYajC[10,11] and YidC.[12] The latter supports either independently[13,14] or in association with SecYEG and SecDFYajC,[15] the integration of membrane proteins.

Several lines of evidence indicate that both SecA and SecYEG can exist in dynamic multimeric associations. In solution, SecA forms a dimer under physiological conditions,[16,17] and it was shown to be active in translocation as a dimer.[18] On the basis of the observation that liposomes containing anionic phospholipids induce the monomerization of SecA, it was suggested that it may dissociate into monomers during translocation.[19] However, other findings indicated that the dimeric form of SecA is restored upon interaction with the signal peptide domain of preproteins questioning the monomerization of SecA in its active state.[20]

Solubilized *E. coli* SecYEG exhibits a detergent concentration-dependent monomer–dimer equilibrium.[21] At higher concentrations of protein, larger oligomers are formed.[21,22] In negatively stained preparations of solubilized *E. coli* SecYEG, 2-fold symmetric, dimeric assemblies of 6.7 nm width and 8.7 nm length with a 2 nm wide stain-filled indentation appear.[23] Similarly, the solubilized SecYE complex of *Bacillus subtilis*[24] and the homologous eucaryotic Sec61p have been described as oligomeric ring-like structures, the latter having 8.5 nm diameter and a central pore with a diameter of 1.5–2.0 nm.[25,26] SecYEG forms dimers in lipid bilayers, as demonstrated for the SecYE complex of the thermophilic bacterium *Thermus thermophilus HB8* by fluorescence resonance energy transfer (FRET) analysis,[27] and for the *E. coli* SecYEG by electron crystallography.[22,28] The electron density map at about 8 Å in-plane resolution obtained from two-dimensional crystals of *E. coli* SecYEG shows an arrangement of dimers with a cavity of 1.6–2.5 nm width and 2.2 nm depth at the dimer interface. This cavity is closed on the periplasmic side by two highly tilted transmembrane helices that correspond to the TM3 of SecE. In this respect, the structure resembles the eukaryotic ribosome–nascent chain–Sec61 complex that contains a central indentation closed on the lumenal side of the membrane.[29] The crystal structure of the Sec61 complex from the archaeon *Methanococcus jannaschii* at 3.2 Å resolution contains a single copy of the heterotrimer, with a molecular architecture nearly identical with that of the *E. coli* SecYEG complex.[30] At the cytoplasmic side, the rectangular heterotrimer shows a 2.0–2.5 nm funnel-like cavity, which is closed in the middle of the membrane by a constriction with bulky hydrophobic amino acid residues, and closed at the periplasmic side of the membrane by a loop-structure connecting transmembrane segments 1 and 2.

Despite the determination of the high-resolution structure of the SecYEG complex, its oligomeric state in the active translocation channel is currently a subject of controversy. Based on immunoprecipitation and cross-linking studies,[31] blue native PAGE analysis[32] and the crystal structure of Sec61 complex from *M. jannaschii*,[30] it was suggested that one copy of the SecYEG heterotrimer serves as a functional translocation channel. Cross-linking studies[21] and antibody-stabilization of solubilized subcomplexes,[33] as well as the structure of *E. coli* SecYEG obtained from two-dimensional crystals,[28] implied that the active translocation complex consists of dimeric SecYEG. On the other hand, electron microscopic studies revealed the formation of larger SecYEG assemblies upon interaction with SecA: the species solubilized from SecYEG proteoliposomes upon treatment with SecA and AMP-PNP contained a fraction of SecYEG tetramers with a side-length of 10.5–12 nm with a central, stain-filled indentation of about 5 nm diameter.[23] Mass analysis by scanning transmission electron microscopy on a detergent-solubilized translocase harbouring an arrested preprotein translocation intermediate confirmed that the actual protein-conducting channel may consist of one SecA dimer and four SecYEG heterotrimers.[23] Similarly, the ring-like structures of the eukaryotic Sec61p complex observed in membranes upon incubation with ribosomes with or without nascent polypeptide chains or the Sec62/63p complex are thought to be composed of three or four Sec61 heterotrimers.[26] Cryo-electron microscopy and three-dimensional reconstruction of soluble assemblies consisting of ribosomes and Sec61 complexes have revealed oligomeric Sec61 complexes with a diameter of 8.5 nm, and a 1.5–3.5 nm wide channel that aligns with the nascent-chain tunnel of the large ribosomal subunit.[34] This channel was shown to widen up to 4–5 nm diameter under translocation conditions.[35]

All biochemical studies reported so far addressing the oligomeric state of *E. coli* SecYEG in the active state were performed on complexes that were solubilised from translocating proteoliposomes or inner membrane vesicles. Given the probability that some of the interactions stabilizing higher-order structures may occur only in the membrane, insight into the oligomeric composition and dynamics of SecYEG assemblies while they are still embedded in the membrane is crucial for understanding the mechanism of channel formation. Thus, we performed FRET and freeze-fracture experiments to study the quaternary structure of SecYEG after reconstitution into liposomes, and examined the distribution of SecYEG oligomers under non-translocating and translocating conditions. The data show that SecYEG can exist in different multimeric associations in lipid bilayers, and exchange of SecYEG subunits occurs between oligomers. In addition, freeze-fracture experiments indicate that the formation of higher oligomers is favoured in the presence of membrane-inserted SecA or of translocation ligands. These data support the oligomerisation model of the active translocation channel.

Results

Functional reconstitution of cysteine-labelled SecYEG into liposomes

Solubilized *E. coli* SecYEG exists in a monomer–dimer equilibrium,[21,23] while larger oligomers are formed at high concentrations of protein.[21,22] We used FRET to determine whether different oligomeric associations of SecYEG exist also in lipid bilayers. For fluorescence measurements, proteoliposomes containing SecYEG labelled with maleimide derivatives of Oregon green or Texas red at unique cysteine residues at position Ile96 or Ser120 in SecE were used. The cysteine residues in solubilized SecYE(I96C)G (Figure 1(a)) and SecYE(S120C)G (data not shown) could be labelled specifically under conditions that allowed only weak labelling of Cys-less SecYEG. The efficiency of labelling was in the range of 70–90% (data not shown). Purified and labelled SecYEG was reconstituted into liposomes and tested for its ability to support proOmpA-stimulated SecA ATPase activity. This demonstrated that the presence of the fluorescent dye in SecE does not affect the translocation ATPase activity (Figure 1(b)).

Energy transfer reveals SecYEG oligomerization in a lipid environment

To determine possible oligomer formation, donor (Oregon green) and acceptor (Texas red)-labelled SecYEG were mixed in a 1:1 ratio either before or after reconstitution into liposomes. In the first case, donor and acceptor fluorophores are co-localized within the same liposomes, while in the latter case, donor and acceptor fluorophores are localized in separated liposomes. Fluorescence emission scans were recorded with the excitation wavelength set at the excitation maximum of Oregon green (480 nm). A significantly lower fluorescence was observed at the emission maximum of Oregon Green for both SecYE(I96C)G and SecYE(S120C)G when the donor and acceptor fluorophores were co-localized as compared to conditions where the donor alone was present, or the donor and acceptor were present in separate liposomes (Figure 2). For SecYE(I96C)G, the decrease in Oregon green emission is accompanied by an increase in fluorescence around 610 nm representing the Texas red emission (Figure 2(a)). This indicates clearly the occurrence of resonance energy transfer, and demonstrates that the two probes are in close proximity. In the case of SecYE(S120C)G, only a quenching of the Oregon green fluorescence was observed (Figure 2(b)). However, this was dependent on the presence of Texas red-labelled SecYE(S120C)G and not observed with non-labelled SecYEG (data not shown). Oregon green labelled SecYE(S120C)G proteoliposomes were also mixed with Texas red-labelled SecYE(S120C)G proteoliposomes in a 1:1 ratio and fused by a freeze/thaw and sonication treatment. The emission scan reveals that this treatment also results in lower Oregon green emission fluorescence (Figure 2(c)). Further FRET analysis of the oligomeric state of SecYEG in the presence of translocation ligands was complicated by the observation

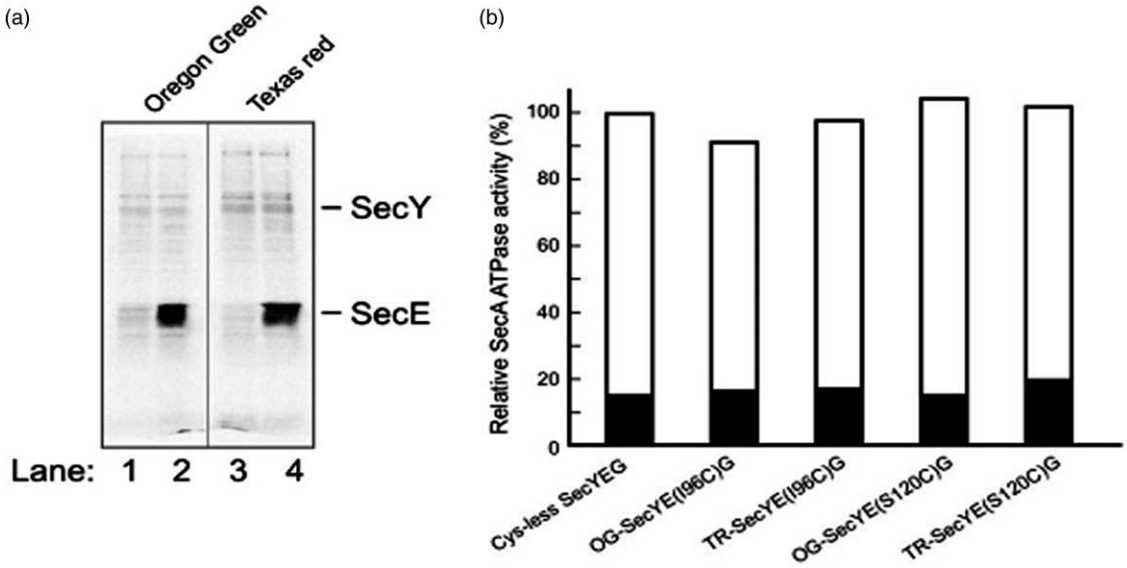

Figure 1. (a) Cysteine-specific labelling of SecYE(I96C)G. Cys-less SecYEG (lanes 1 and 3) and SecYE(I96C)G (lanes 2 and 4) were purified and labelled with Oregon green (lanes 1 and 2) and Texas red maleimide (lanes 3 and 4). The fluorescence was visualized after loading the samples onto an SDS gel (15% polyacrylamide) using a Roche Lumi-Imager F1 with a high-pass filter with a cutoff at 520 nm for Oregon green and 600 nm for Texas red. (b) ProOmpA stimulated SecA ATPase activity. Oregon green (OG) and Texas red (TR)-labelled SecYE(I96C)G and SecYE(S120C)G were reconstituted into proteoliposomes and the SecA ATPase activity in the presence (open bars) and in the absence (filled bars) of proOmpA was determined. The activity of proteoliposomes harboring Cys-less SecYEG was set to 100%.

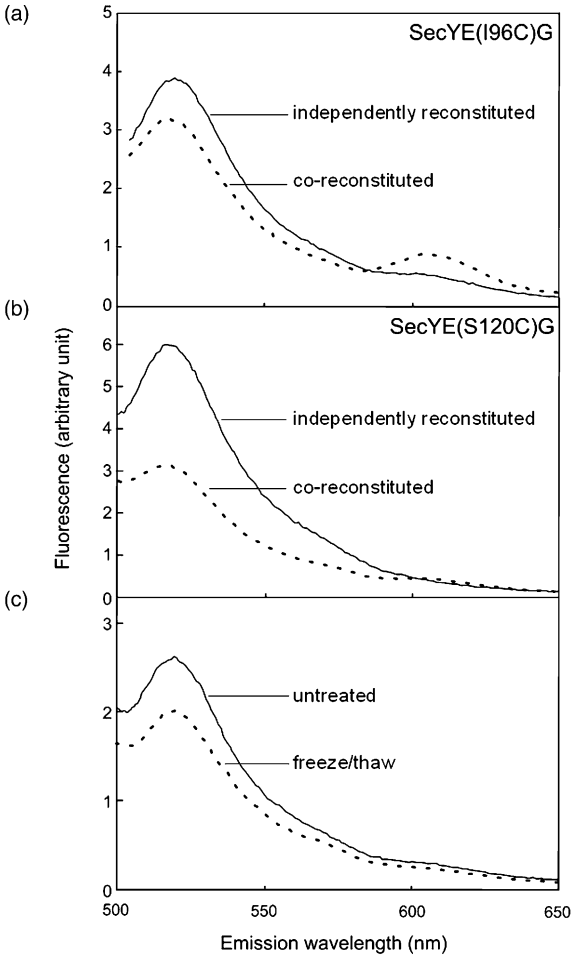

Figure 2. FRET analysis of SecYEG reconstituted into proteoliposomes. Fluorescence spectra of proteoliposomes containing Oregon green (donor) and Texas red (acceptor)-labelled (a) SecYE(I96C)G or (b) SecYE(S120C)G. Spectra represent 1:1 mixtures of Oregon green and Texas Red-labelled SecYEG that were co-reconstituted (dotted line) or independently reconstituted (continuous line) into proteoliposomes. The excitation wavelength was set to 480 nm. (c) Fluorescence spectra of a 1:1 mixture of Oregon green and Texas red-labelled SecYE(S120C)G proteoliposomes before (continuous line) and after (dotted line) a freeze/thaw treatment and sonication to fuse the proteoliposomes. The excitation wavelength was set to 480 nm.

that the Oregon green fluorescence was quenched significantly upon addition of SecA (data not shown). Taken together, these data demonstrate that SecYEG assembles into an oligomeric form when embedded in the membrane.

Oligomeric forms of SecYEG in proteoliposomes

To determine the oligomeric distribution of SecYEG in lipid bilayers quantitatively, SecYEG proteoliposomes reconstituted at various lipid to protein ratios (LPR) were tested for activity by measuring their preprotein-stimulated SecA translocation ATPase activity and analysed by freeze-fracture electron microscopy. Unidirectional shadowing with Pt/C revealed on the hydrophobic cleavage planes well-defined, large particles as well as smaller ones (Figure 3). The particle size distribution depended largely on the lipid to protein ratio. At low concentrations of protein (LPR > 10, (w/w)), the ratio of small to large particles was in the range of 1.5–2.5, while at higher concentrations of protein (LPR < 5), the ratio was approximately 0.6. The increase in particle size with increasing protein concentration suggests the self-association of SecYEG heterotrimers into well-defined oligomers.

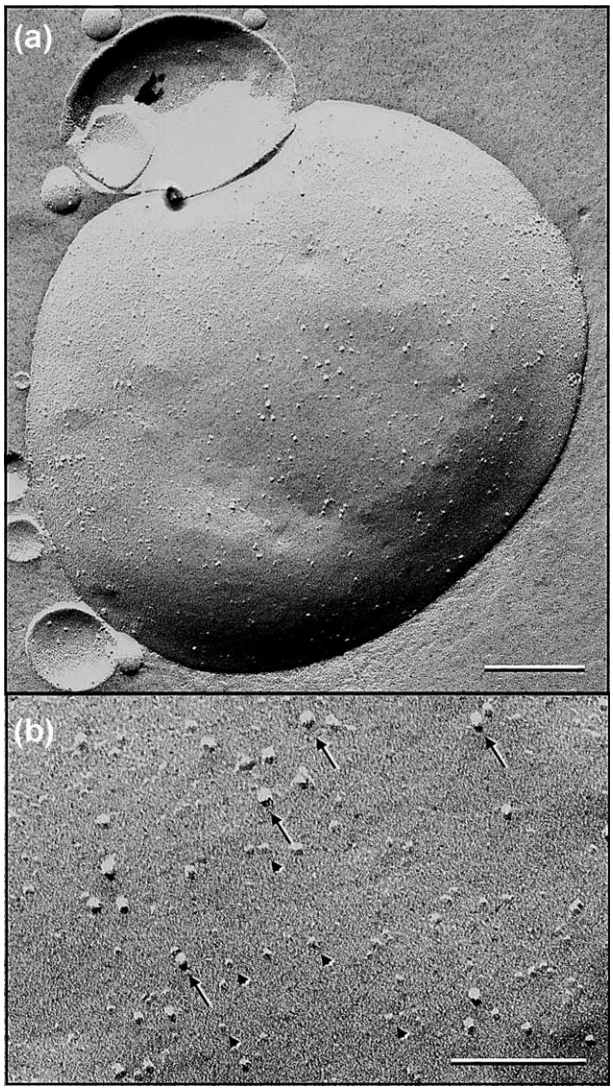

Figure 3. Electron micrograph of freeze-fractured and Pt/C-shadowed proteoliposomes (*E. coli* lipids, LPR 10) with reconstituted *E. coli* SecYEG (shadowing angle 30°, film thickness 1.4 nm). (a) Overview (the scale bar represents 200 nm); (b) the same as (a) but at higher magnification. Large particles with a diameter of ~ 10 nm are indicated by long arrows, the smaller particles (diameter ~ 5 nm) are indicated by short arrows (the scale bar represents 100 nm).

To characterize the morphology and the size of the oligomers, SecYEG proteoliposomes reconstituted at LPR 7 were freeze-fractured and rotationally shadowed with Pt/C. Electron micrographs showed a large number of ring-like structures with heterogeneous size distribution (Figure 4). For image analysis, particles from flat membrane areas were selected manually, self-centred, and subjected to multi reference alignment (MRA) using circular references with diameters ranging from 5 nm to 12 nm. The analysis revealed two major particle populations (classes I and II) and a less-populated and thus less-defined third class (class III) (Figure 5(a)). The populations differed significantly in their apparent average outer diameters as determined from radial density distributions (Figure 5(c)) and in their metal distribution. The average diameter of particles in class I was 6.4 nm, in class II it was 8.4 nm, and in class III it was 11.7 nm. As particles may appear larger in rotational shadowing due to the thickness of the evaporated material, and no correction for the metal thickness was made, the values may represent upper estimates for particle diameters. In addition, global averages of populations containing some elongated particles may have larger apparent dimensions due to the lack of rotational alignment during the MRA. Nevertheless, since the observed particle sizes were in good agreement with monomeric, dimeric and tetrameric SecYEG species within the above limitations (Table 1), we concluded that *E. coli* SecYEG exists in proteoliposomes in a monomer–dimer–tetramer equilibrium. Under the experimental conditions, the oligomeric distribution corresponded to 56.2% monomers, 42.4% dimers and 1.4% tetramers (Figure 5(b)).

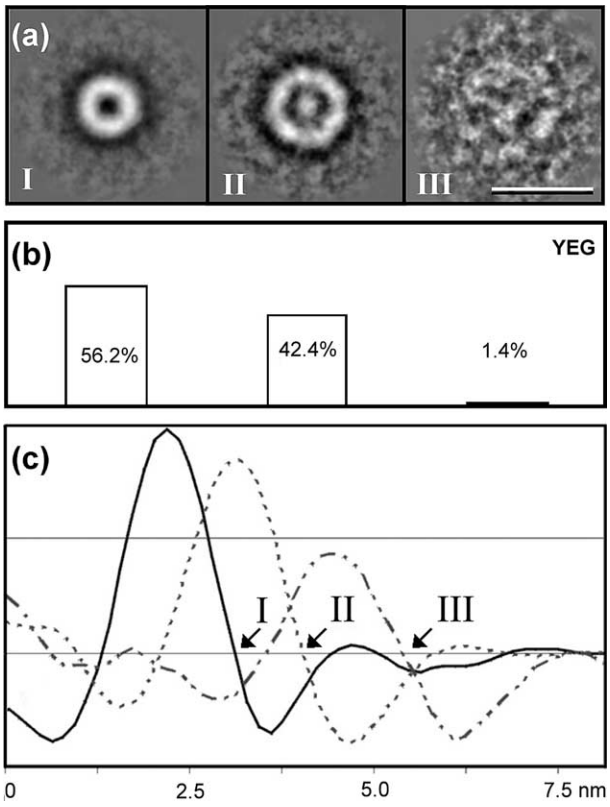

Figure 5. Major particle populations in SecYEG proteoliposomes obtained upon classification with respect to their diameters. (a) Global averages of the size classes I–III with diameters of 6.4 nm, 8.4 nm and 11.7 nm, respectively (the scale bar represents 10 nm). (b) Distribution of the particles among the size classes. (c) Radial density distributions of the size classes I–III. Cylindrically averaged densities were calculated from the averaged images and plotted against the radius.

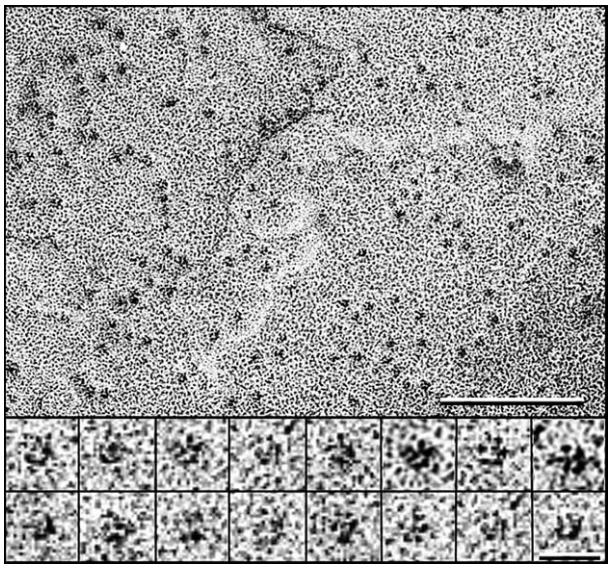

Figure 4. Electron micrograph of proteoliposomes containing *E. coli* SecYEG reconstituted at LPR 7, freeze-fractured and rotationally shadowed (Pt/C, 25°, 0.9 nm). Overview (the scale bar represents 100 nm) with a gallery of enlarged single particles (the scale bar represents 10 nm).

To characterize the morphologies of SecYEG oligomers, individual size classes were subjected independently to cycles of multivariate statistical analysis (MSA) and rotational alignment. The subsequent classification resulted in the major class averages shown in Figure 6(a). The two class averages Ia and Ib corresponding to monomeric SecYEG (Figure 6(a)) have slightly different shapes: whereas Ia is more or less ring-like with a diameter of 6.2 nm, Ib is rectangular with a width of 5.4 nm and a length of 6.5 nm. Due to the bidirectional reconstitution of SecYEG into liposomes, the two class averages may represent periplasmic and cytoplasmic views of the SecYEG complex. Although our data do not allow an *a priori* assignment of the observed classes to either face of the complex, comparison with the three-dimensional map of *E. coli* SecYEG obtained from two-dimensional crystals[28] suggests that the rectangular class average Ib in Figure 6(a) represents the view from the cytoplasmic face of

Table 1. Calculated and measured surface areas for monomeric, dimeric and tetrameric SecYEG

	SecYEG	$(SecYEG)_2$	$(SecYEG)_4$
Molecular mass (kDa)	75	150	300
Surface area (nm^2) calculated from:			
Molecular mass[a]	15.4	30.8	61.5
α-Helices[b]	27	54	108
Surface area (nm^2) measured in:			
2D crystals[c]	28	55.5	–
Negatively stained preparations of solubilized complexes[d]	30.6	59.1	110–125
Freeze-fracturing[e]	32 (class I)	55 (class II)	107 (class III)
d (nm) measured in freeze-fracturing	6.4	8.4	11.7

[a] Minimum surface area calculated for a cylindrical molecule with an estimated height of 6 nm and a density of 1.35 g/cm^3 without correction for the lipid content and a putative pore.
[b] Surface areas calculated for 15, 30 and 60 membrane-spanning α-helices with an estimated surface area of 180 $Å^2$ per α-helix.
[c] From Breyton *et al*.[28]
[d] From Manting *et al*.[23]
[e] Surface areas calculated from the diameters of the global class averages after MRA without correction for the metal thickness, SecYEG proteoliposomes.

the complex. The monomer dimensions viewed from the cytoplasmic face of the crystallographic dimer correspond to approximately 5 nm width and 6.5 nm length, which fits well with the observed width and length of 5.4 nm and 6.5 nm, respectively. In negatively stained preparations of solubilized *E. coli* SecYEG,[23] monomeric SecYEG species were viewed only as rectangular particles with 4.5 nm width and 6.8 nm length presumably due to the adsorption of the complex onto carbon grids in this specific orientation. Taking into account that the particle dimensions from freeze-fracture experiments represent overestimates, and that the solubilized complexes appear larger due to the bound detergent micelles (Table 1), the values from freeze-fracture and negative staining experiments agree very well.

The class averages IIa and IIb corresponding to dimeric SecYEG (Figure 6(a)) both show ring-like shapes with an average diameter of 8.3 nm,

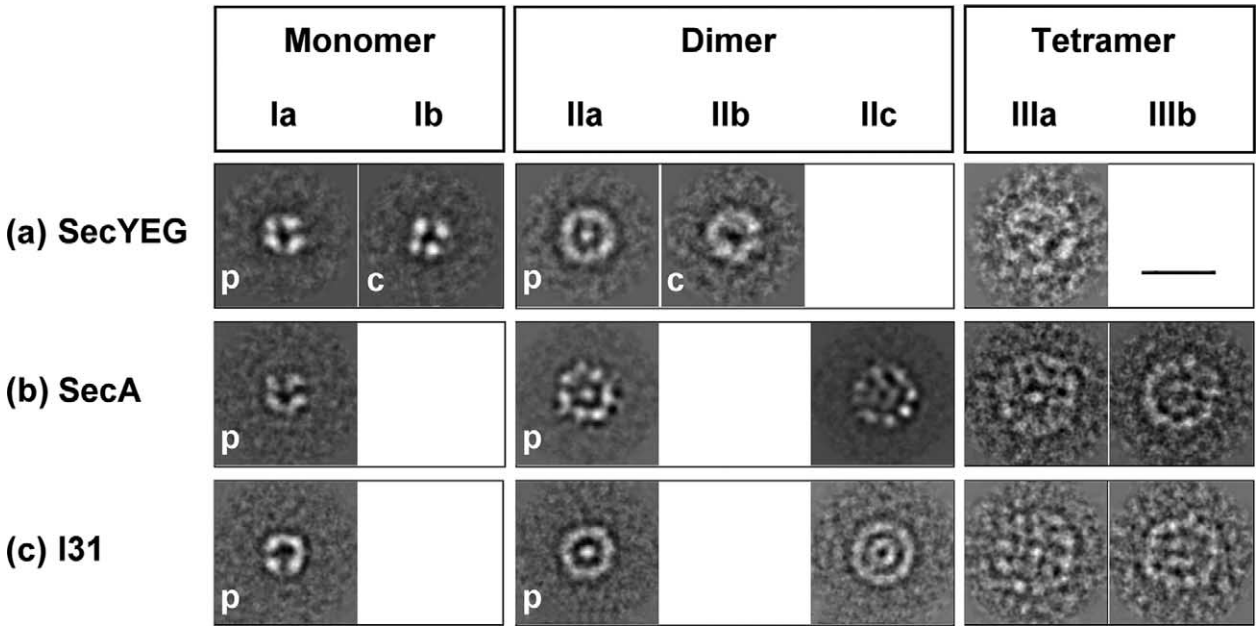

Figure 6. Major class averages of reconstituted SecYEG in various experiments obtained by MSA of rotationally shadowed particles. Classes that resemble each other are listed in the same column. (a) SecYEG (SecYEG alone): Ia and Ib, class averages of the monomeric population (520 particles analysed); IIa and IIb, class averages of the dimeric population (393 particles analysed); IIIa, tetrameric species (global average). (b) SecA (SecYEG proteoliposomes upon incubation with SecA and AMP-PNP): Ia, class average of the monomeric population (225 particles analysed); IIa and IIc, class averages of the dimeric population (1230 particles analysed); IIIa and IIIb, class averages of the tetrameric population (137 particles analysed). (c) I31 (SecYEG proteoliposomes harboring the translocation intermediate I_{31}: Ia, class average of the monomeric population (621 particles analysed); IIa and IIc, class averages of the dimeric population (1223 particles analysed); IIIa and IIIb, class averages of the tetrameric population (69 particles analysed). p, periplasmic view; c, cytoplasmic view. The scale bar represents 10 nm.

which is in accordance with the observations from electron microscopy[23] and electron crystallography (Table 1).[28] The two classes differ significantly, however, in their internal structures, as judged from the metal distribution. The averaged density in class average IIa shows significant accumulation of metal in its centre, while the density in the central part of the class average IIb is much lower than the surrounding background. This suggests that the top and bottom views differ in their surface reliefs: whereas one face shows a partially occluded cavity or a less-pronounced depression, the other contains a deep indentation or an open pore. The three-dimensional map of the *E. coli* SecYEG dimer, which is organized as a back-to-back dimer, shows a 22 Å deep cavity at the interface of the monomers that is closed on the periplasmic membrane surface.[28] Thus, it seems likely that the class averages IIa and IIb correspond to the periplasmic and the cytoplasmic views of the SecYEG dimer, respectively.

Due to the limited number of tetrameric SecYEG species in the population, the corresponding class averages were very noisy and did not show any additional structural features as compared to the global average obtained by MRA (Figure 5(a), class IIIa).

Oligomeric distribution of reconstituted SecYEG upon incubation with SecA and AMP-PNP

To determine whether the oligomeric distribution of SecYEG is affected upon interaction with SecA, SecYEG proteoliposomes (LPR 7) were incubated with SecA in the presence of the non-hydrolysable ATP analogue AMP-PNP, which enforces membrane insertion of SecA even when preprotein is not present.[5] Prior to freezing, SecA and AMP-PNP-treated proteoliposomes were analysed by SDS-PAGE, which demonstrated the association of almost all SecA protein with the proteoliposomes. The proteoliposomes were then freeze-fractured and replicated by rotational shadowing with Pt/C. On electron micrographs, a large number of particles with ring-like morphology were found. Analysis of these structures with respect to particle sizes by MRA revealed three major classes (Figure 7(a)). The particle diameters of 6.6 nm in class average I, 9.1 nm in class average II and 12.0 nm in class average III indicated again the presence of monomeric, dimeric and tetrameric SecYEG. The average diameters of all three populations were only slightly larger (3–8%) than those observed in SecYEG proteoliposomes. Most strikingly, however, the overall distribution of the oligomers changed significantly when compared to the oligomer distribution in untreated SecYEG proteoliposomes. In SecA and AMP-PNP pre-incubated proteoliposomes, the monomeric SecYEG fraction contributed to only 14.1% of the whole population while the dimer and the tetramer fractions contributed to 77.3% and 8.6%, respectively (Figure 7(b)). The observed shifts clearly suggest the formation of higher oligomers from SecYEG monomers and/or dimers upon interaction with AMP-PNP and SecA. AMP-PNP was essential for the oligomerization, as proteoliposomes incubated only with SecA contained mainly particles corresponding to monomeric and dimeric SecYEG (data not shown).

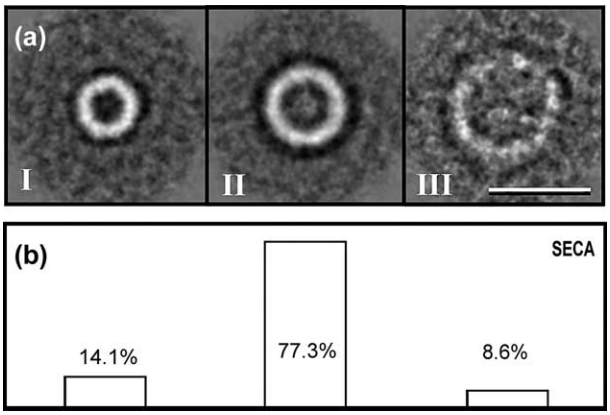

Figure 7. Major particle populations in SecYEG proteoliposomes upon incubation with SecA and AMP-PNP obtained by MRA. (a) Global averages of the size classes I–III with approximate diameters of 6.6 nm, 9.1 nm and 12.0 nm, respectively. The diameters were determined from radial density distributions (the scale bar represents 10 nm). (b) Distribution of the particles among the size classes.

To test whether SecA itself forms ring-like structures upon adsorbtion on lipid layers, as has been reported,[36] we analysed liposomes of *E. coli* lipids that were incubated with SecA or SecA/AMP-PNP by freeze-fracture electron microscopy. However, no ring-like structure was observed on the replicas.

The individual size classes of SecA and AMP-PNP-treated SecYEG particles were subjected independently to MSA and classified (Figure 6(b)). In contrast to SecYEG proteoliposomes, the monomer population contained only one well-defined structure with a more or less ring-like shape and a diameter of 6.3 nm (Figure 6(b), class Ia). There was no evidence for the existence of the rectangular monomeric form that was found in untreated SecYEG proteoliposomes (Figure 6(a), class Ib). This further supports the interpretation that the rectangular monomer corresponds to the cytosolic face of SecYEG. Interestingly, a non-negligible part (about 30%) of the monomer particles showed a great variation in size (±15%) and form, so that their assignment to a specific class was not possible. These particles may correspond to monomeric SecYEG with associated SecA. It is unclear, however, why they lack distinct structural features. The dimeric SecYEG species grouped into two representative subpopulations (Figure 6(b), classes IIa and IIc). The class IIa with a diameter

of 8.5 nm and significant accumulation of metal in the centre of the particle was strikingly similar to the class average obtained from SecYEG containing proteoliposomes (Figure 6(a), class IIa). However, a dimer population with low metal density in the central part of the particle could not be found. Interestingly, the metal distribution in class IIc (Figure 6(b)) with an average diameter of 9.6 nm indicated a complex surface relief that was significantly different from that of the dimer class averages observed in SecYEG proteoliposomes. The disappearance of the dimer population with low metal density, and the appearance of the novel particle type upon incubation of SecYEG with SecA and AMP-PNP suggest that this particle represents a dimeric SecYEG-SecA bound species that is assembled upon membrane insertion of SecA. A similar surface relief was observed on one of the class averages of tetrameric SecYEG population (Figure 6(b), class IIIb), which was not indicated in SecYEG proteoliposomes. In analogy, and because of the shifted distribution, these particles may correspond to tetrameric SecYEG species assembled upon recruitment by SecA. The other tetrameric SecYEG subpopulation (Figure 6(b), class IIIa) displayed accumulation of metal in its centre and, in this respect, resembled the dimeric class IIa (Figure 6(b)). As the tetramer class averages were fuzzy, their size could be estimated only to approximately 12 nm.

Translocase-precursor complex

To determine the oligomeric distribution of SecYEG in a translocation-active state, we analysed proteoliposomes harbouring a preprotein translocation intermediate (I_{31}). The translocation intermediate was prepared by incubation of SecYEG proteoliposomes (LPR 7) with SecB, SecA, ATP and proOmpA under oxidizing conditions. In the absence of reducing agents, proOmpA is arrested in the translocase due to an internal disulfide bridge at the C terminus, which prevents complete translocation.[23] To control the formation of the intermediate I_{31}, the translocation ATPase activity was monitored during the incubation of the sample (Figure 8) using the spectrophotometric assay.[37] The ATPase activity reached its maximum within approximately 15 minutes of incubation at 37 °C and then remained nearly constant at the level of lipid-stimulated ATPase activity of SecA, presumably due to the block of the active translocation sites by I_{31} (Figure 8). Similar observations have been reported by Schiebel *et al.*,[6] who employed a colorimetric assay for ATPase activity. Upon addition of DTT to a final concentration of 10 mM, an increase of the ATPase activity was observed, indicating new cycles of translocation (Figure 8).

Prior to freezing, SecA/SecB/ATP/proOmpA-treated proteoliposomes were analysed by SDS-PAGE, which demonstrated the association of the major portion of SecA and precursor with the proteoliposomes (data not shown). Subsequent

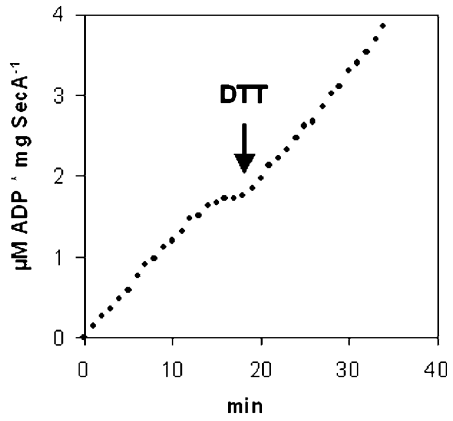

Figure 8. Formation of the translocation intermediate I_{31}. Proteoliposomes containing reconstituted SecYEG (20 µg/ml) were mixed in the absence of DTT with 20 µg/ml of SecB, 20 µg/ml of SecA, 50 µg/ml of proOmpA and 1 mM ATP at 37 °C. The formation of I_{31} was followed by monitoring the translocation ATPase activity. DTT at a final concentration of 10 mM was added (arrow) after I_{31} reached its maximum and remained nearly constant at the level of lipid-stimulated ATPase activity of SecA.

freeze-fracturing and rotational shadowing resulted in a heterogeneous particle population. Analysis by MRA indicated the existence of monomeric (class I), dimeric (class II) and tetrameric (class III) SecYEG (Figure 9(a)). The diameters were estimated from global averages to be 6.3 nm for monomeric, 9.1 nm for dimeric and 12.4 nm for tetrameric SecYEG, which contributed to 32.5%, 63.9% and 3.6% of the whole population, respectively (Figure 9(b)). The

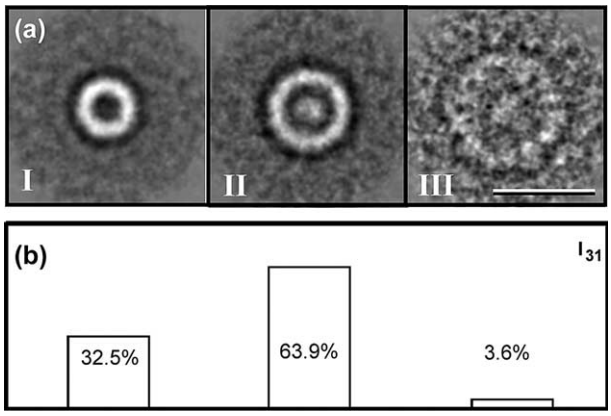

Figure 9. Major particle populations obtained by MRA of particles observed in freeze-fractured and rotationally shadowed SecYEG proteoliposomes harbouring the translocation intermediate I_{31}. (a) Global averages of the size classes I–III with approximate diameters of 6.3 nm, 9.1 nm and 12.4 nm, respectively. A total of 1913 particles was analysed. The diameters were determined from radial density distributions (the scale bar represents 10 nm). (b) Distribution of the particles among the size classes.

increase in the number of dimeric and tetrameric particles compared to the oligomer distribution in SecYEG proteoliposomes again suggests the formation of higher oligomers from SecYEG monomers and/or dimers under conditions that yield the translocation intermediate I_{31}. The less pronounced preference for oligomer formation compared to proteoliposomes with membrane-inserted SecA may be due to a less complete translocation reaction. Alternatively, the deinsertion of SecA may partly cause the disassembly of oligomeric SecYEG channels leaving smaller building blocks associated with the preprotein. Nevertheless, the results demonstrate that the oligomerization of SecYEG is triggered in the presence of translocation ligands SecA, preprotein and ATP.

Upon MSA of the monomeric SecYEG populations, no evidence could be found for the presence of elongated, monomeric SecYEG particles. The representative class presented ring-like particles with a diameter of approximately 6.2 nm (Figure 6(c), class Ia). Interestingly, a significant fraction of monomeric particles (approximately 40%) differed in their relief properties from the species observed in the former two experiments. On these particles, the distribution of metal slightly indicated a double-ring structure. However, large variations in their size and shape did not allow their accurate alignment and led to a fuzzy average (data not shown). The classification of the dimeric and tetrameric SecYEG populations indicated again the formation of new dimeric and tetrameric species with surface characteristics very similar to those formed upon membrane insertion of SecA (Figure 6(c)), although the tetramer averages were noisy. It is likely that the inserted preprotein is too small to induce relief effects of sufficient magnitude to be disclosed by rotational shadowing. Thus, the possibility cannot be excluded that subtle structural differences may exist between these species formed under different conditions. However, the results suggest the same underlying mechanism for their formation.

Cytosolic membranes

For the visualization of SecYEG protein in its native environment, inside out (ISO) membrane vesicles of SecYEG overexpressing and control *E. coli* strains were analysed by freeze-fracturing and rotational shadowing. Ring-like structures similar to those observed on reconstituted SecYEG proteoliposomes were found on native ISO vesicles from overexpressing cells. However, the complexity of the native membrane vesicles did not allow a detailed image analysis (data not shown).

Discussion

The oligomeric state of SecYEG in the active protein-conducting channel of the *E. coli* translocation apparatus has been addressed in numerous biochemical studies utilizing complexes solubilized from translocating proteoliposomes or inner membrane vesicles. Although the various studies proposed differing stoichiometries for the active translocon, several lines of evidence have emerged suggesting a dynamic nature for the translocation channel and the possibility that different SecYEG assemblies exist during the translocation process. A dynamic channel structure would imply weak associations of the protomers, which may lead to the dissociation of the SecYEG complexes during detergent solubilisation and purification. Thus, we have used FRET and freeze-fracture electron microscopy to elucidate the oligomeric compositions of SecYEG assemblies embedded in lipid bilayers. Our data demonstrate that membrane-embedded SecYEG exists in a concentration-dependent equilibrium between monomers, dimers and tetramers. The formation of dimers and tetramers is, however, significantly stimulated by membrane insertion of SecA and by the interaction with SecA and preprotein supporting the oligomer model of the active translocation channel.

As a model system, we have used proteoliposomes with reconstituted SecYEG that catalyse multiple rounds of preprotein translocation[38] as well as insertion of hydrophobic transmembrane proteins into the lipid bilayer.[39] In FRET experiments, a significant loss in donor (Oregon green) emission fluorescence occurred when populations of donor and acceptor fluorophore-labelled SecYE(I96C)G complexes were co-localized in the same liposome environment. This demonstrates that SecYEG heterotrimers are in close proximity. High concentrations of donor and acceptor-labelled proteins in the liposomes could lead to random transient contacts and thus possibly result in energy transfer. However, the typical molar protein to lipid ratio for SecYEG reconstituted proteoliposomes used in these studies is ~1:4000 (LPR 40 (w/w)) and under these conditions energy transfer by non-specific contacts can be ruled out.[27] We therefore conclude that the observed energy transfer demonstrates association of SecYEG complexes into oligomers in proteoliposomes. Furthermore, donor quenching was observed when donor and acceptor-labelled SecYEG, originally in separate populations of liposomes, were co-localized after liposome fusion. This suggests a dynamic exchange of subunits between oligomers of SecYEG in the liposome environment. Our finding contradicts the FRET data for the SecYE complex from *T. thermophilus*, which suggested no apparent exchange of subunits.[27] In these experiments, SecY was labelled but, since SecY and SecE do not dissociate *in vivo*,[40] it is unlikely that the difference can be explained by an exchange of SecE subunits. Possibly, the higher physiological temperature, the lack of an SecG homologue, or the fact that the *T. thermophilus* SecYE complex was reconstituted into *E. coli* liposomes cause a significantly slower exchange rate of subunits for the *T. thermophilus* SecYE complex.

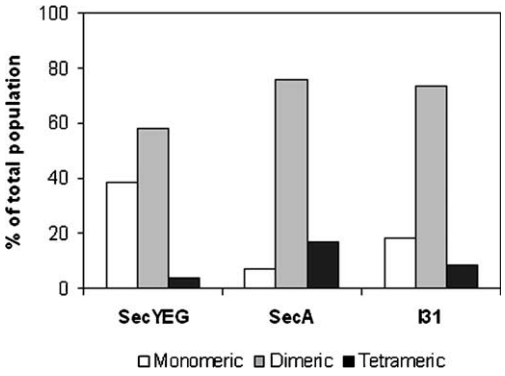

Figure 10. The percentage of SecYEG heterotrimers organized as monomers, dimers and tetramers in proteoliposomes containing SecYEG, membrane-inserted SecA and the translocation intermediate I_{31} (I31). The total number of heterotrimers was calculated from the distribution among the size classes, i.e. the distribution into monomeric (one heterotrimer), dimeric (two heterotrimers) and tetrameric (four heterotrimers) complexes as shown in Figures 5(b), 7(b) and 9(b), respectively.

Freeze-fracture analyses reveal a concentration-dependent monomer–dimer–tetramer distribution for SecYEG in the lipid bilayer. Proteoliposomes reconstituted at LPR 7 display an oligomer distribution corresponding to approximately 56% monomers, 42.5% dimers and 1.5% tetramers, demonstrating that the majority of SecYEG (approximately 60%) is organized as a dimer (Figure 10). In line with our observations, a monomer–dimer–tetramer distribution has been reported for SecYEG solubilized from inner membrane vesicles of an approximately tenfold overexpressing *E. coli* strain[21] with a SecYEG content comparable to that in proteoliposomes reconstituted at LPR 7. The formation of tetramers or even higher oligomers has been attributed to the unnaturally high SecYEG concentrations in proteoliposomes or in overexpressing membranes.[21,31] We cannot exclude this possibility, as we have no data on the oligomeric distribution of SecYEG in native membranes, but our data indicate a SecA and AMP-PNP-dependent shift in the distribution of these oligomeric species, demonstrating that their presence is not simply the result of an overexpression but rather caused by interactions with translocation ligands. Image analysis of rotationally shadowed proteoliposomes revealed cytosolic and periplasmic faces of both monomeric and dimeric SecYEG species in the lipid bilayer, consistent with the bi-directional reconstitution of SecYEG into proteoliposomes. The particle dimensions for all species observed in proteoliposomes were in accordance with the observations from electron microscopy[23] and electron crystallography.[28] Interestingly, the particles corresponding to the periplasmic face of the SecYEG dimer in the lipid bilayer showed drastic variations in their diameters up to 15% which are not likely to arise from different film thicknesses due to the variations in the angle of incidence of the evaporated metal as the analysed particles were chosen from flat membrane areas. A similar phenomenon was reported for the SecYE complex of *Bacillus subtilis*,[24] and for the eukaryotic Sec61p complex,[26] and attributed to an inherent degree of structural flexibility of the complexes. The variations in *E. coli* SecYEG dimer dimensions may also correspond to different conformational states of the dimeric complex; however, it remains unclear why this structural plasticity is not reflected on its cytoplasmic face.

Our results demonstrate unambiguously that membrane insertion of SecA triggers the recruitment of SecYEG protomers to form oligomers, which is evident in the substantial increase of the total amount of dimeric and tetrameric SecYEG species. Upon incubation of SecYEG proteoliposomes with SecA and AMP-PNP, 76% of the SecYEG heterotrimers become trapped in dimers and 17% in tetramers (Figure 10) implying that the fraction of the SecYEG heterotrimers incorporated into dimers is, compared to untreated SecYEG proteoliposomes, increased by about 30%. More remarkably, the fraction incorporated into tetramers is increased by more than 200%, underlining tetramer assembly as the predominant process. These results are consistent with the former observations by electron microscopy and mass measurements on solubilised SecYEG assemblies upon membrane insertion of SecA: the species solubilised from SecYEG proteoliposomes upon treatment with SecA and AMP-PNP contained, next to a dimeric fraction, a substantial amount of SecYEG tetramers.[23] Similar to the bacterial system, the homologous eukaryotic Sec61p complex also assembles into larger complexes composed of multiple Sec61 heterotrimers upon incubation with ribosomes or with Sec62/63p.[26] Contrary to our observations, a chemical cross-linking approach gave no evidence for changes in the overall distribution of the oligomeric forms of the SecYEG upon AMP-PNP driven SecA membrane insertion. However, the same crosslinker was shown to interfere with oligomerisation, as assayed by blue native PAGE.[21] A recent study using antibody-stabilized SecA–SecYEG complexes in detergent solution provided evidence for an AMP-PNP-induced stable complex of dimeric SecA and dimeric SecYEG.[33] Additional evidence for the enzymological event that occurs upon membrane insertion of SecA came from the structures that were observed in proteoliposomes incubated with SecA and AMP-PNP. First, the particles assigned to the active cytoplasmic faces of monomeric and dimeric SecYEG species disappear upon reaction with SecA, and the non-reactive periplasmic monomer and dimer faces remain unaltered in their size and shape, consistent with the fact that only the cytosolic faces of SecYEG complexes can specifically react with SecA. Second, upon reaction with membrane inserted SecA, dimeric and tetrameric SecYEG particles with novel structural

properties emerge, giving further support to the hypothesis that they have assembled upon membrane insertion of SecA. These reaction products also exhibit larger outer diameters compared to dimeric and tetrameric SecYEG particles in the lipid bilayer without any treatment. From the surface images, however, we cannot conclude whether these species formed upon the enzymatic event contain SecA in the inserted state.

The oligomeric distribution of SecYEG in lipid bilayers is modulated strongly by the presence of translocation ligands SecA, preprotein and ATP. In proteoliposomes where a translocating preprotein is trapped in the active translocase (I_{31}), the amounts of dimeric and tetrameric SecYEG increase significantly compared to the oligomeric distribution of SecYEG in untreated proteoliposomes. This is consistent with the data obtained by electron microscopy and scanning transmission electron microscope measurements of solubilised complexes,[23] which corroborate the formation of dimeric and tetrameric SecYEG assemblies with associated SecA under conditions yielding the translocation intermediate. According to our analysis, in proteoliposomes with translocase–I_{31} complexes, approximately 73% of the SecYEG heterotrimers are organized in dimers and 8% in tetramers (Figure 10). Compared to the oligomeric distribution in SecYEG proteoliposomes, these numbers correspond to an increase in the fraction of monomers trapped in dimers and of those trapped in tetramers by 26% and 100%, respectively, again emphasizing the tetramer formation as a prevailing process. On the other hand, when compared to the oligomeric distribution of SecYEG in proteoliposomes containing membrane-inserted SecA, the oligomerization appears less efficient. Most strikingly, the monomeric SecYEG population in proteoliposomes with translocation intermediate I_{31} contain a significant fraction of particles with rather vague structural properties that could not be assigned to any of the monomeric SecYEG classes found in the former experiments. Altogether, the observations raise the possibility that the increase in the monomer fraction is due to the disassembly of tetrameric species upon deinsertion of SecA leaving monomers associated with the preprotein. Earlier immunoprecipitation and cross-linking studies,[31] as well as blue native PAGE analysis,[32] indicated a stable association of an arrested preprotein with monomeric SecYEG in detergent solution and thus suggested that a minimal stable form of the preprotein translocase is monomeric SecYEG. Our analysis, and that performed by blue native PAGE,[32] does not allow us to distinguish between active and non-active species in the bilayer and therefore does not allow for conclusions to be reached about the oligomeric state of SecYEG in the active translocon. However, at this stage of the analysis, we consider it more likely that the monomeric SecYEG particles with less-defined characteristics observed in proteoliposomes harbouring the translocation intermediate represent dissociation products rather than stable particle associations, as these would display distinct structural properties.

Our results demonstrate that ligand-triggered changes in oligomeric interactions between SecYEG protomers in the membrane may play a functional role during the complex translocation reaction. Upon membrane insertion of SecA, as well as upon interaction with translocation ligands, dimeric and tetrameric SecYEG assemblies with different channel sizes form and coexist in the membrane. This is consistent with the observations on the homologous eukaryotic system: translocating microsomal membranes contain two distinct Sec61p populations with a pore size of either 0.9–1.5 nm or 4–6 nm, which may indicate different Sec61p oligomeric states.[41]

Materials and Methods

Materials

E. coli phospholipids were purchased from Avanti Polar Lipids (Alabaster, AL). *n*-Dodecyl-β-D-maltoside (DDM) was from CalBiochem (San Diego, CA). Rabbit lactate dehydrogenase and rabbit pyruvate kinase were from Sigma. Oregon green® 488 maleimide, Texas red® maleimide and tris-(2-carboxyethyl)phosphine (TCEP) were from Molecular Probes (Leiden, The Netherlands). Stock solutions of 40 mM Oregon green and Texas red were prepared in dimethylformamide (DMF) and dimethylsulfoxide (DMSO), respectively. SOURCE-30Q column material and HiTrap chelating HP columns were from Amersham Biosciences (Freiburg, Germany).

Plasmids

pET607 (cysteine-less SecYEG),[42] pET2501 (SecYE(I96C)G),[43] and pET2523 (SecYE(S120C)G) were used to overexpress His_6-tagged SecYEG. pET2523 was constructed in a similar manner as pET2501 and its cysteine mutation (*secE* A120C (TCC→TGT)) was confirmed by sequence analysis.

Protein overexpression and purification

E. coli SecA,[44] SecB,[45] proOmpA[46] and SecYEG were overexpressed and purified as described.[47,48]

Cysteine labelling of SecYEG

Semi-purified fractions after anion-exchange chromatography were pooled and incubated with a twofold molar excess of TCEP for 15 min at 4 °C. Subsequently, a tenfold molar excess of Oregon green or Texas red maleimide was added. Labelling was carried out at pH 8.0 for 60 min at 4 °C. The reaction was quenched for 15 min at 4 °C by the addition of a 20-fold molar excess of reduced glutathione. The Ni-chelating purification step was used to remove unbound dye. Labelling specificity was analysed after SDS-PAGE (15% (w/v) acrylamide), followed by visualization of in gel fluorescence on a Roche Lumi-Imager F1. Subsequently, the gel was stained with Coomassie brilliant blue to evaluate the purification steps.

Preparation of SecYEG proteoliposomes

For freeze-fracture experiments, solubilized SecYEG (0.3 mg/ml) in 100 mM imidazole buffer (pH 7.0), 100 mM KCl, 0.2% DDM, 20% glycerol and *E. coli* lipids (20 mg/ml, solubilized in 2% DDM) were mixed in the appropriate LPR and incubated for 20 min on ice. Polystyrol beads (BioBeads SM2-Adsorbent, BioRad) were added at 100 mg per 1 ml of reconstitution mixture stepwise in 30 min intervals while stirring on ice. The mixture was stored overnight on ice and diluted threefold with 50 mM Tris–HCl (pH 8.0), 50 mM KCl. Proteoliposomes were harvested by centrifugation in a 70 Ti Rotor (Beckman Instruments) at 45,000 rpm at 4 °C for 1 h, and resuspended in 50 mM Tris–HCl (pH 8.0), 50 mM KCl, tested for their translocation ATPase activity and frozen in aliquots at −18 °C. For FRET experiments, fluorescence-labelled SecYEG was reconstituted by rapid dilution as described.[47]

SecYEG/SecA/AMP-PNP complex

SecYEG-containing proteoliposomes (80 μg of SecYEG /ml, LPR 7) and *E. coli* SecA (400 μg /ml) were mixed in a total volume of 250 μl of 50 mM Hepes–KOH (pH 7.6), 50 mM KCl, 10 mM magnesium acetate, 2 mM AMP-PNP kept on ice for 5 min, and then incubated at 37 °C for 20 min. Liposomes were concentrated at 44,000 rpm in a TLA-45 rotor in a Beckman Optima 35 Max-E ultracentrifuge for 35 min, resuspended in 20 μl of the supernatant and frozen in liquid ethane for freeze-fracture analysis. For a control, a portion of the proteoliposomes was washed twice with buffer, and both vesicles and supernatant were analysed by SDS-PAGE (12.5% acrylamide). Almost all SecA protein was found in the proteoliposome fraction, indicating its association with the proteoliposomes.

Translocation intermediate I_{31}

The translocation intermediate I_{31}[23] was prepared by mixing 400 μg/ml of SecA, 50 μg/ml of urea-denaturated proOmpA, 50 μg/ml of SecB and SecYEG-containing proteoliposomes (80 μg of SecYEG/ml, LPR 7) in 50 mM Hepes–KOH (pH 7.6), 50 mM KCl, 10 mM magnesium acetate, 2 mM ATP, kept on ice for 5 min, incubated at 37 °C for 30 min. The proteoliposomes were concentrated at 44,000 rpm in a TLA-45 rotor in a Beckman Optima 35 Max-E ultracentrifuge for 35 min, resuspended in 20 μl of the supernatant and frozen in liquid ethane for freeze-fracture analysis. A portion of the proteoliposomes was washed twice with buffer, and both vesicles and supernatant were analysed by SDS-PAGE (12.5% acrylamide). The major portion of SecA and preprotein were found in the proteoliposome fraction, indicating that they were associated with the vesicles. Control experiments to follow the formation of the intermediate by the ATPase activity were performed in the absence of DTT using the spectrophotometric assay described by Hanada *et al.*[37] The assay buffer contained 5 units/ml of pyruvate kinase, 7.5 units/ml of lactate dehydrogenase, 3 mM phosphoenol pyruvate, 0.25 mM NADH, 1 mM ATP, 50 mM Tris–HCl (pH 8.0), 50 mM KCl, 5 mM $MgCl_2$. Assay buffer (500 μl) was mixed with proteoliposomes (20 μg/ml of SecYEG final concentration, LPR 7), sonicated three times for 10 s and preincubated at 37 °C for 5 min. The reaction was started by the addition of 20 μg/ml of SecA, preincubated at 37 °C, and 50 μg/ml of urea-denatured proOmpA. The reaction was monitored by the change of absorption at 340 nm in a temperature-controlled spectrophotometer at 37 °C.

Other biochemical methods

Protein concentrations were determined with the Bio-Rad DC Protein Assay Kit using bovine serum albumin as the standard. ProOmpA-stimulated translocation ATPase assays of the reconstituted SecYEG vesicles were performed by the colorimetric assay as described.[49,50] Fusion of the proteoliposomes was induced by three cycles of freezing in liquid nitrogen and thawing at room temperature, followed by disaggregation by sonication for 10 s in a bath sonicator.

Fluorometry

FRET measurements were performed on an SLM Aminco-Bowman series 2 luminescence spectrometer (SLM Aminco, Urbana, IL) with excitation and emission slit-widths set to 4 nm. Oregon green was excited at 480 nm and emission scans were recorded as indicated in the Figures. Proteoliposomes containing fluorescence-labelled SecYEG were diluted in the cuvette with buffer A (50 mM Tris–HCl (pH 8.0), 50 mM KCl) prior to the measurements. Emission scans of tryptophan fluorescence (excited at 280 nm) were recorded to determine the relative concentration of protein in the proteoliposomes, and the concentration was corrected if necessary.

Electron microscopy

Proteoliposomes were frozen in liquid ethane and fractured at −130 °C in a freeze-etching apparatus BA360 or BAF 400. Freeze-fracture replicas were obtained by either unidirectional shadowing with Pt/C at an angle of incidence of 35° or rotational shadowing at 25°. The film thickness (10–15 Å) was monitored with a quartz crystal oscillator. After coating the specimen with a carbon support film at normal incidence (30–40 Å), the replica was floated on water and mounted on specimen grids for electron microscopic observation. Micrographs were taken at nominal magnifications of 33,000× or 50,000× on a JEOL 100CX transmission electron microscope. Images were recorded on Kodak SO163 films, which were developed for 12 min with full-strength developer Kodak D19.

Image processing and classification

Suitable negatives were digitized with a Flextight densitometer (Imacon, Copenhagen, DK) at a step size of 8 μm (corresponding to 0.16 nm at the specimen level for the negatives with a magnification of 50,000×), and single-particle analysis was performed using SEMPER[51] and IMAGIC-5 software.[52,53] Due to the low density and heterogeneous distribution of the particles, the images were extracted interactively in boxes of 128×128 pixels, linearized, normalized and Fourier-filtered. For translational alignment of the images, a self-centre algorithm was performed during which a rotationally averaged version of each input image is generated, and each input image is then translationally aligned relative to its rotationally averaged counterpart. The images were then subjected to MRA using circular references with diameters ranging from 5 nm to 12 nm, which allowed us to subdivide the heterogeneous particle population into

distinct size classes. To obtain information on the internal structure of the particles, populations of different sizes were independently subjected to repeated cycles of MSA[54] and rotational alignment and class averages were calculated.

Acknowledgements

We thank Johannes Buchner for critical reading of the manuscript. This work was supported by a grant from the Deutsche Forschungsgemeinschaft (SFB 594) to S.W. and to A.D. by the Council for Chemical Sciences of the Netherlands Organization for Scientific Research (CW-NWO) which is subsidized by the Dutch Organization for the Advancement of Scientific Research (NWO).

References

1. Manting, E. H. & Driessen, A. J. M. (2000). *Escherichia coli* translocase: the unraveling of a molecular machine. *Mol. Microbiol.* **37**, 226–238.
2. Driessen, A. J. M., Manting, E. H. & van der Does, C. (2001). The structural basis of protein targeting and translocation in bacteria. *Nature Struct. Biol.* **8**, 492–498.
3. Mori, H. & Ito, K. (2001). The Sec protein-translocation pathway. *Trends Microbiol.* **9**, 494–500.
4. de Keyzer, J., van der Does, C. & Driessen, A. J. M. (2003). The bacterial translocase: a dynamic protein channel complex. *Cell Mol. Life Sci.* **60**, 2034–2052.
5. Economou, A. & Wickner, W. (1994). SecA promotes preprotein translocation by undergoing ATP-driven cycles of membrane insertion and deinsertion. *Cell*, **78**, 835–843.
6. Schiebel, E., Driessen, A. J. M., Hartl, F. U. & Wickner, W. (1991). $\Delta\mu_{H+}$ and ATP function at different steps of the catalytic cycle of preprotein translocase. *Cell*, **64**, 927–939.
7. van der Wolk, J. P., de Wit, J. G. & Driessen, A. J. M. (1997). The catalytic cycle of the *Escherichia coli* SecA ATPase comprises two distinct preprotein translocation events. *EMBO J.* **16**, 7297–7304.
8. Joly, J. C. & Wickner, W. (1993). The SecA and SecY subunits of translocase are the nearest neighbors of a translocating preprotein, shielding it from phospholipids. *EMBO J.* **12**, 255–263.
9. Eichler, J. & Wickner, W. (1997). Both an N-terminal 65-kDa domain and a C-terminal 30-kDa domain of SecA cycle into the membrane at SecYEG during translocation. *Proc. Natl Acad. Sci. USA*, **94**, 5574–5581.
10. Duong, F. & Wickner, W. (1997). Distinct catalytic roles of the SecYE, SecG and SecDFyajC subunits of preprotein translocase holoenzyme. *EMBO J.* **16**, 2756–2768.
11. Duong, F. & Wickner, W. (1997). The SecDFyajC domain of preprotein translocase controls preprotein movement by regulating SecA membrane cycling. *EMBO J.* **16**, 4871–4879.
12. Scotti, P. A., Urbanus, M. L., Brunner, J., de Gier, J. W. L., von Heinje, G., van der Does, C. *et al*. (2000). YidC, the *Escherichia coli* homologue of mitochondrial Oxa1p, is a component of the sec translocase. *EMBO J.* **19**, 542–549.
13. Samuelson, J. C., Chen, M., Jiang, F., Moller, I., Wiedmann, M., Kuhn, A. *et al*. (2000). YidC mediates membrane protein insertion in bacteria. *Nature*, **405**, 637–641.
14. van der Laan, M., Bechtluft, P., Kol, S., Nouwen, N. & Driessen, A. J. M. (2004). F_1F_0 ATP synthase subunit c is a substrate of the novel YidC pathway for membrane protein biogenesis. *J. Cell Biol.* **165**, 213–222.
15. Nouwen, N. & Driessen, A. J. M. (2002). SecDFyajC forms a heterotetrameric complex with YidC. *Mol. Microbiol.* **44**, 1397–1405.
16. Woodbury, R. L., Hardy, S. J. & Randall, L. L. (2002). Complex behavior in solution of homodimeric SecA. *Protein Sci.* **11**, 875–882.
17. Ding, H., Hunt, J. F., Mukerji, I. & Oliver, D. (2003). *Bacillus subtilis* SecA ATPase exists as an antiparallel dimer in solution. *Biochemistry*, **42**, 8729–8738.
18. Driessen, A. J. M. (1993). SecA, the peripheral subunit of the *Escherichia coli* precursor protein translocase, is functional as a dimer. *Biochemistry*, **32**, 13190–13197.
19. Or, E., Boyd, D., Gon, S., Beckwith, J. & Rapoport, T. (2005). The bacterial ATPase SecA functions as a monomer in protein translocation. *J. Biol. Chem.* **280**, 9097–9105.
20. Benach, J., Chou, Y. T., Fak, J. J., Itkin, A., Nicolae, D. D., Smith, P. C. *et al*. (2003). Phospholipid-induced monomerization and signal-peptide-induced oligomerization of SecA. *J. Biol. Chem.* **278**, 3628–3638.
21. Bessonneau, P., Besson, V., Collinson, I. & Duong, F. (2002). The SecYEG preprotein translocation channel is a conformationally dynamic and dimeric structure. *EMBO J.* **21**, 995–1003.
22. Collinson, I., Breyton, C., Duong, F., Tziatzios, C., Schubert, D., Or, E. *et al*. (2001). Projection structure and oligomeric properties of a bacterial core protein translocase. *EMBO J.* **20**, 2462–2471.
23. Manting, E. H., van der Does, C., Remigy, H., Engel, A. & Driessen, A. J. M. (2000). SecYEG assembles into a tetramer to form the active protein translocation channel. *EMBO J.* **19**, 852–861.
24. Meyer, T. H., Ménétret, J. F., Breitling, R., Miller, K. R., Akey, C. W. & Rapoport, T. A. (1999). The bacterial SecY/E complex forms channel-like structures similar to those of eucaryotic Sec61p complex. *J. Mol. Biol.* **285**, 1789–1800.
25. Hartmann, E., Sommer, T., Prehn, S., Görlich, D., Jentsch, S. & Rapoport, T. A. (1994). Evolutionary conservation of the components of the protein translocation complex. *Nature*, **367**, 654–657.
26. Hanein, D., Matlack, K. E. S., Jungnickel, B., Plath, K., Kalies, K. U., Miller, K. R. *et al*. (1996). Oligomeric rings of the Sec61p complex induced by ligands required for protein translocation. *Cell*, **87**, 721–732.
27. Mori, H., Tsukazaki, T., Masui, R., Kuramitsu, S., Yokoyama, S., Johnson, A. E. *et al*. (2003). Fluorescence resonance energy transfer analysis of protein translocase. SecYE from *Thermus thermophilus* HB8 forms a constitutive oligomer in membranes. *J. Biol. Chem.* **278**, 14257–14264.
28. Breyton, C., Haase, W., Rapoport, T. A., Kühlbrandt, W. & Collinson, I. (2002). Three-dimensional structure of the bacterial protein-translocation complex SecYEG. *Nature*, **418**, 662–665.

29. Beckmann, R., Spahn, C. M. T., Eswar, N., Helmers, J., Penczek, P. A., Sali, A. *et al*. (2001). Architecture of the protein-conducting channel associated with the translating 80S ribosome. *Cell*, **107**, 361–372.
30. van den Berg, B., Clemons, W. M., Jr, Collinson, I., Modis, Y., Hartmann, E., Harrison, S. C. & Rapoport, T. A. (2004). X-ray structure of a protein-conducting channel. *Nature*, **427**, 36–44.
31. Yahr, T. L. & Wickner, W. (2000). Evaluating the oligomeric state of SecYEG in preprotein translocase. *EMBO J.* **19**, 4393–4401.
32. Duong, F. (2003). Binding, activation and dissociation of the dimeric SecA ATPase at the dimeric SecYEG translocase. *EMBO J.* **22**, 4375–4384.
33. Tziatzios, C., Schubert, D., Lotz, M., Gundogan, D., Betz, H., Schägger, H. *et al*. (2004). The bacterial protein translocation complex: SecYEG dimers associate with one or two SecA molecules. *J. Mol. Biol.* **340**, 513–524.
34. Beckmann, R., Bubeck, D., Grassucci, R., Penczek, P., Verschoor, A., Blobel, G. & Frank, J. (1997). Alignment of conduits for the nascent polypeptide chain in the ribosome-Sec61 complex. *Science*, **278**, 2123–2126.
35. Hamman, B. D., Chen, J. C., Johnson, E. E. & Johnson, A. E. (1997). The aqueous pore through the translocon has a diameter of 40–60 Å during the cotranslational protein translocation at the ER membrane. *Cell*, **89**, 535–544.
36. Wang, H.-W., Chen, Y., Yang, H., Chen, X., Duan, M.-X., Tai, P. C. & Sui, S.-F. (2003). Ring-like pore structures of SecA: implication for bacterial protein-conducting channels. *Proc. Natl Acad. Sci. USA*, **100**, 4221–4226.
37. Hanada, M., Nishiyama, K., Mizushima, S. & Tokuda, H. (1994). Reconstitution of an efficient protein translocation machinery comprising SecA and the three membrane proteins, SecY, SecE and SecG (p12). *J. Biol. Chem.* **269**, 23625–23631.
38. Bassilana, M. & Wickner, W. (1993). Purified *Escherichia coli* preprotein translocase catalyses multiple cycles of precursor protein translocation. *Biochemistry*, **32**, 2626–2630.
39. van der Laan, M., Nouwen, N. & Driessen, A. J. M. (2004). SecYEG proteoliposomes catalyze the $\Delta\psi$-dependent membrane insertion of FtsQ. *J. Biol. Chem.* **279**, 1659–1664.
40. Joly, J. C., Leonard, M. R. & Wickner, W. T. (1994). Subunit dynamics in *Escherichia coli* preprotein translocase. *Proc. Natl Acad. Sci. USA*, **91**, 4703–4707.
41. Hamman, B. D., Hendershot, L. M. & Johnson, A. E. (1998). BiP maintains the permeability barrier of the ER membrane by sealing the lumenal end of the translocon before and early in translocation. *Cell*, **92**, 747–758.
42. Kaufmann, A., Manting, E. H., Veenendaal, A., Driessen, A. J. M. & van der Does, C. (1999). Cysteine-directed cross-linking demonstrates that helix 3 of SecE is close to helix 2 of SecY and helix 3 of a neighboring SecE. *Biochemistry*, **38**, 9115–9121.
43. Veenendaal, A. K. J., van der Does, C. & Driessen, A. J. M. (2001). Mapping the sites of interaction between SecY and SecE by cysteine scanning mutagenesis. *J. Biol. Chem.* **276**, 32559–32566.
44. Cabelli, R. J., Chen, L., Tai, P. C. & Oliver, D. B. (1988). SecA protein is required for secretory protein translocation into *E. coli* membrane vesicles. *Cell*, **55**, 683–692.
45. Weiss, J. B., Ray, P. H. & Bassford, P. J., Jr (1988). Purified SecB protein of *Escherichia coli* retards folding and promotes membrane translocation of the maltose-binding protein in vitro. *Proc. Natl Acad. Sci. USA*, **85**, 8978–8982.
46. Crooke, E., Guthrie, S., Lecker, S., Lill, R. & Wickner, W. (1988). ProOmpA is stabilized for membrane translocation by either purified *E. coli* trigger factor or canine signal recognition particle. *Cell*, **54**, 1003–1011.
47. van der Does, C., Manting, E. H., Kaufmann, A., Lutz, M. & Driessen, A. J. M. (1998). Interaction between SecA and SecYEG in micellar solution and formation of the membrane-inserted state. *Biochemistry*, **37**, 201–210.
48. van der Does, C., Swaving, J., van Klompenburg, W. & Driessen, A. J. M. (2000). Non-bilayer lipids stimulate the activity of the reconstituted bacterial preprotein translocase. *J. Biol. Chem.* **275**, 2472–2478.
49. Lanzetta, P. A., Alvarez, L. J., Reinach, P. S. & Candia, O. A. (1979). An improved assay for nanomole amounts of inorganic phosphate. *Anal. Biochem.* **100**, 95–97.
50. Lill, R., Dowhan, W. & Wickner, W. (1990). The ATPase activity of SecA is regulated by acidic phospholipids, SecY, and the leader and mature domains of precursor protein. *Cell*, **60**, 271–280.
51. Saxton, W. O., Pitt, T. J. & Horner, M. (1979). Digital image processing: the SEMPER system. *Ultramicroscopy*, **4**, 343–354.
52. van Heel, M. & Keegstra, W. (1981). Imagic: a fast, flexible and friendly image analysis software system. *Ultramicroscopy*, **7**, 113–130.
53. van Heel, M., Harauz, G., Orlova, E. V., Schmidt, R. & Schatz, M. (1996). A new generation of IMAGIC image processing system. *J. Struct. Biol.* **116**, 17–24.
54. van Heel, M. & Frank, J. (1981). Use of multivariate statistics in analysing the images of biological macromolecules. *Ultramicroscopy*, **6**, 187–194.

Edited by W. Baumeister

(Received 3 June 2005; received in revised form 30 August 2005; accepted 20 September 2005)
Available online 7 October 2005